A donor-acceptor Stenhouse adduct displaying reversible photoswitching in water and neuronal activity

Rossella Castagna[†‡¶], Galyna Maleeva[†], Deborah Pirovano[†], Carlo Matera[†‡#], Pau Gorostiza[†‡§]*

† Institute for Bioengineering of Catalonia (IBEC), The Barcelona Institute for Science and Technology (BIST), Baldiri Reixac 10-12, 08028 Barcelona, Spain

‡ Network Biomedical Research Center in Bioengineering, Biomaterials and Nanomedicine (CIBER-BBN), Spain

§ Catalan Institution for Research and Advanced Studies (ICREA), Barcelona, Spain

¶ Present affiliation: Latvian Institute of Organic Synthesis, Aizkraukles 21, Riga 1006, Latvia

 # Present affiliation: Department of Pharmaceutical Sciences, University of Milan, 20133 Milan, Italy

* pau@icrea.cat

Keywords: donor–acceptor Stenhouse adducts, photoswitch; photochromism; photochemistry; solvatochromism; red light; cyclodextrin; cage-complex

Abstract

The interest in the photochromism and functional applications of donor-acceptor Stenhouse adducts (DASAs) soared in recent years, owing to their outstanding advantages and flexible design. However, their low solubility and irreversible conversion in aqueous solutions hampered exploring DASAs for biology and medicine. It is notably unknown whether the barbiturate electron acceptor group retains the pharmacological activity of drugs like phenobarbital, which targets γ-aminobutyric acid (GABA) type A receptors ($GABA_ARs$) in the brain. Here, we have developed the model compound DASA-barbital based on a scaffold of red-switching second-generation DASAs and we demonstrate that it is active in $GABA_ARs$ and alters the neuronal firing rate in physiological medium at neutral pH. DASA-barbital can also be reversibly photoswitched in acidic aqueous solutions using cyclodextrin, an approved ingredient of drug formulations. These findings clear the path towards the biological applications of DASAs and to exploit the versatility displayed in polymers and materials science.

Introduction

Donor-acceptor Stenhouse adducts (DASAs) are an alluring class of photochromic compounds that can be efficiently switched using visible and near-infrared (NIR) light[1,2], display high absorption coefficient, high conversion rate[3], and great flexibility of design. The linear triene colored form is thermally stable and is reversibly photoconverted to a cyclic colorless form (Figure 1) which has about half the size, a remarkably different geometry, and higher polarity.[2] As the photoproduct is colorless (T-type negative photochromism) and does not absorb the excitation light, conversion of the molecule enhances light penetration and thus propagates from the surface into the bulk of the material. The backward reaction is thermally activated and takes place in the dark on different time scales, which depend on the solvent and on the chemical features of the molecule[4,5].

Their use in chemistry and materials science is favoured by the fact that polymer chains can be functionalized with DASA molecules to endow them with photoswitchable properties. This approach enabled creating artificial nanosystems such as polymersome nanoreactors[4], photopatterning of polymer surfaces,[6] and polymer dots for thermal- and chemo-sensors.[7,8] These compounds have also been used to irreversibly release drugs with light for nanomedicine.[9,10] The broad range of reported applications of DASAs has been reviewed recently[5,11] and continues to grow.

The DASA switching mechanism has been elucidated combining experimental and theoretical approaches, revealing its intermediate steps and the guidelines to design DASA photoswitches[12–14]. These studies have identified different isomerization and rotation steps, followed by an electrocyclization and proton transfer mechanism that leads to the final cyclized form of the compound.[13] DASA compounds absorb red light because of their highly conjugated push-pull structure and planar backbone, which shifts their absorption to wavelengths up to 750 nm[15]. Their accessible synthetic route has enabled developing a library of DASA derivatives with variable donors,[15,16] acceptors,[17] and spacer linkers[18,19] to customize physicochemical and photochromic properties. The cyclic compound obtained by photoconversion sets apart the first and subsequent generations of DASAs. In the first generation,[2] the donor moiety features a secondary aliphatic amine, which results in a zwitterionic cyclic-colorless photoproduct. In the second[15] and third[17] generations, the use of an aniline donor moiety yields mainly nonzwitterionic photoproducts. This modification has expanded the potential applications of DASA photoswitches: first generation DASAs can be photoisomerized only in nonpolar solvents, whereas later generation DASAs can be reversibly switched also in organic polar solvents and polymer matrices.[15]

The isomerization process depends on the solvent, temperature, chemical substituents, and

concentration[4,20–22] but low solubility and spontaneous and irreversible conversion of the linear form into the cyclic form are unavoidably observed in water.[15,23,24]

The hurdles to operate DASAs in aqueous solutions are most aggravating since they are native red/NIR-absorbing, negative photochromic compounds that would afford low scattering and deep penetration in tissue without incurring phototoxicity in biological applications[25]. These properties are appealing for photopharmacology, which aims at controlling drug action on demand at selected locations using light, to enable precise responses and reduce unwanted side effects of treatments, or to manipulate specific cell types and neural circuits for investigational purposes.[26,27] Many photoswitchable bioactive molecules have been reported that offer high pharmacological specificity and potency for a diversity of targets, including ion channels[28–30], G protein-coupled receptors[31–33] and enzymes[34–37]. Most are based on aryl azo compounds[38–40], which are difficult to isomerize using orange-red light without introducing substituents that often perturb the pharmacological properties of the original compound.[41–43] Photoswitching with continuous NIR light has been achieved in diazocines[42] and using two-photon (2P) excitation of simple azobenzenes[32,44,45] in neurons but the latter requires pulsed lasers and precision optics[46,47]. Thus, developing compounds that can be directly photoswitched *in vivo* with continuous-wave red or NIR light using portable devices (e.g. LEDs) remains an unmet need in basic and applied photopharmacology. They would enable noninvasive drug-based phototherapies and facilitate their translation to the clinic.

DASAs offer unique opportunities in that respect because (1) they intrinsically photoisomerize with long-wavelength light and (2) the barbiturate moiety that acts as electron acceptor also constitutes the pharmacologically active group in essential drugs like phenobarbital[48] and pentobarbital (Figure 1a),[49] which target γ-aminobutyric acid (GABA) type A receptors ($GABA_ARs$). These ion channels hyperpolarize the cell membrane and inhibit action potential firing in neurons upon binding of GABA, thereby mediating inhibitory neurotransmission in the mammalian central nervous system and playing central roles in nociception, memory formation, and cognition[50]. However, the intriguing question of whether the barbiturate moiety of DASAs retains $GABA_AR$-binding properties has never been addressed.

We developed the model compound DASA-barbital (Figure 1b) based on a scaffold of red-switching second-generation DASAs[15] and we demonstrate that it can be solubilized and reversibly photoswitched in aqueous solution using the molecular cage cyclodextrin, an approved excipient in drug formulations. We also show for the first time that DASA-barbital is active in neurons and that its effects are mediated by $GABA_ARs$. These results may be applicable to other DASAs and bear relevance for clinical applications of photopharmacology.

Results

The DASA scaffold is amenable to rationally design red-switching barbiturate ligands.

Molecular design. We examined whether the barbiturate electron-acceptor group DASAs[1] matches the pharmacophoric properties of $GABA_AR$ allosteric potentiators[51]. Single N-alkylation of barbiturates increases their lipid solubility, shortens the duration of drug action, and strengthens their antiepileptic properties, whereas alkylation at both nitrogen atoms causes convulsive effects[52]. Clinically approved barbiturates are unsubstituted (barbital, phenobarbital) or have one methylated nitrogen (methylphenobarbital) (Figure 1a). In principle, non-substituted nitrogens of the barbituric acid are compatible with its role as acceptor group in a Stenhouse scaffold because they do not affect the energy barrier for the ring-closing reaction and thus preserve the photoswitching process[53]. For simplicity, we kept both –NH groups free as a trade-off between photochromic performance, synthetic accessibility, and $GABA_AR$ binding.

The hypnotic and anticonvulsant pharmacological activity of barbiturates also requires the addition of a side chain to the barbituric acid. All clinically approved barbiturate drugs feature branched alkyl chains and/or bulky aryl groups (Figure 1a). The pharmacophore thus appears generally compatible with the DASA scaffold. Branched substitutions were not included as they would disrupt photoswitching at this position. Besides, the photochromic properties of the molecule can be adjusted by introducing aromatic rings as donor groups in the structure that bathochromically shift its absorption peak towards the far visible-red region of the spectrum, as featured in the second and third generation DASA molecules.[15,17] We chose the indoline group because it is reported to provide good photoswitching efficiency and to extend the conjugation of the molecule in the linear form leading to absorption maxima above 600 nm,[15] all desirable properties in photopharmacology.[38,54]

Synthesis. DASA-barbital has a good synthetic accessibility and can be prepared in two steps following a pathway similar to that described for its parent DASA compound bearing a 1,3-dimethyl malonylurea[15] (Figure 1b). The barbituric acid−furan adduct (**1**) can be prepared in near-quantitative yield by reacting a mixture of barbituric acid and 2-furaldehyde in water at room temperature. Several solvents and reaction times were tested to optimize the conditions for the ring-opening reaction with the secondary aniline (indoline). All the organic solvents typically used for this reaction, like tetrahydrofuran, acetonitrile and dimethylformamide, gave low yields probably due to the low solubility of the malonyl urea (Figure 1c). In contrast, DASA-barbital (**2**) was obtained in sufficient yield by stirring a solution of **1** and indoline in methanol for 4 hours. The ratios between linear-DASA-barbital and cyclic-DASA-barbital forms in the dark and after illumination were determined by ^{1}H NMR analysis.

Freshly prepared deuterated dimethylsulfoxide (DMSO-d_6) solutions of the solid compound kept in the dark showed a 68:32 ratio between the linear:cyclic forms, in agreement with the ratio reported for the dimethylated reference molecule[5]. Upon illumination with a wide-spectrum halogen lamp (peak emission at 600-700 nm), the mixture composition was inverted and displayed a 24:76 ratio (Figure 1d).

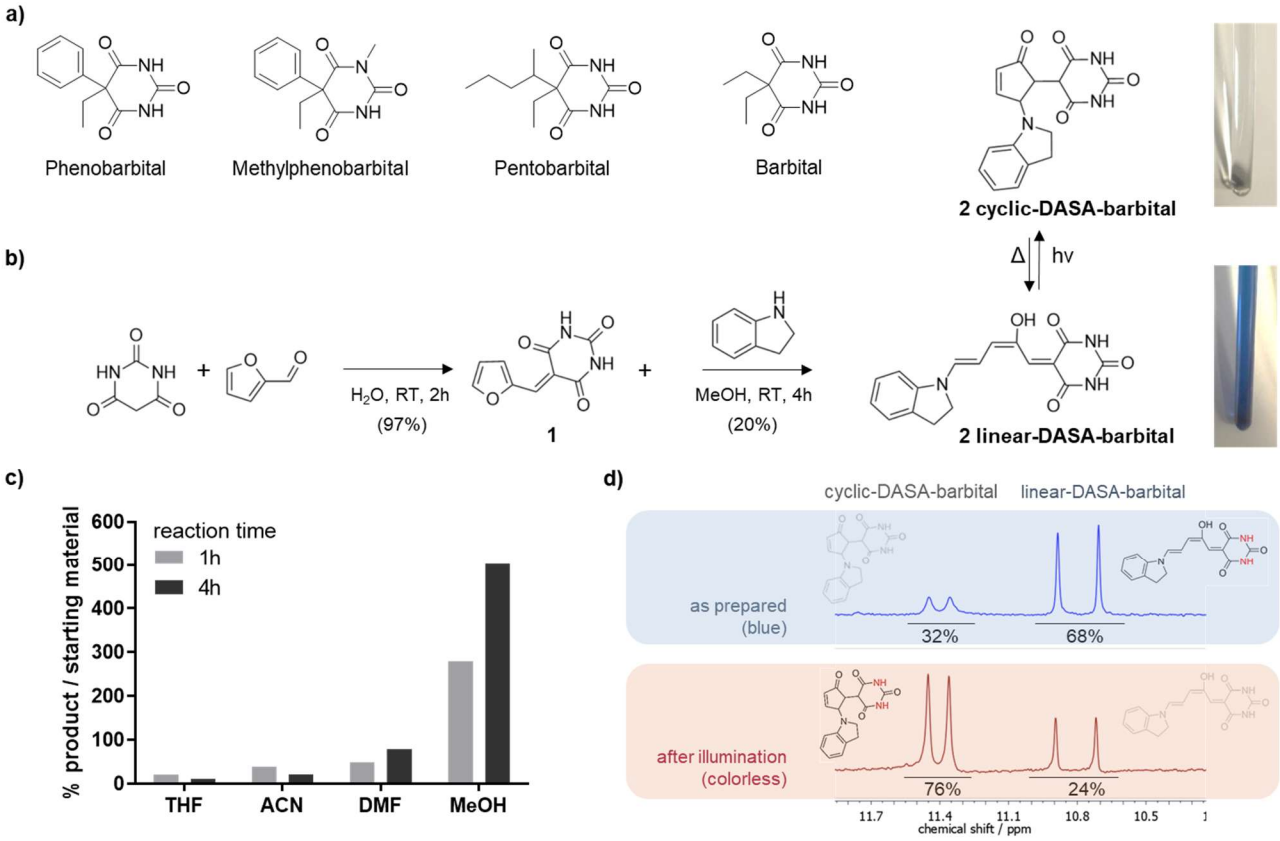

Figure 1. Synthesis and characterization of DASA-barbital. a) Chemical structure of $GABA_AR$-binding barbiturates (phenobarbital, methylphenobarbital, pentobarbital, barbital) that inspired the design of DASA-barbital (right). **b)** Synthetic route of DASA-barbital and chemical structure of its two isomers: linear-DASA-barbital (blue in DMSO) isomerizes to cyclic-DASA-barbital (colorless in DMSO) by absorption of light and spontaneously reverts back to the linear, colored form. **c)** Course of reaction in different solvents expressed as the ratio between product and starting material (in %) measured by peak integration of HPLC chromatograms after a reaction time of 1 h and 4 h. **d)** Composition of the compound mixture (linear and cyclic forms were identified by ^{1}H-NMR analysis, DMSO-d_6) before and after 10 min illumination with a 150 W halogen lamp (broad emission band between 600-700 nm).

DASA-barbital can be reversibly photoswitched in water using a pharmaceutical excipient.

The UV-vis absorption spectrum of DASA-barbital in DMSO (Figure 2a) shows a narrow absorption band around 615 nm that is consistent with the bright blue color of the solution (Figure 1). Upon

illumination, the absorption band decreases as the molecule switches from the colored linear form to the colorless cyclic form. In the dark and at room temperature, the molecule spontaneously converts back to the linear form. The absorption peak after 100 min is recovered by half (exponential time constant, tau ½ = 17 min) and the composition is stable for at least 180 min after recovery (Figure 2b and Figure S6 and S10).

However, in water (pH 8, 50 μM, 0.5% DMSO) DASA-barbital undergoes a spontaneous and irreversible fast conversion from the linear to the cyclic form (exponential time constant, tau ½ = 2.6 min) (Figure 2c and Figure S11). This behavior prevents controlling the photoswitching of the compound and is generally reported for DASA switches.[5] The stability of linear-DASA-barbital can be improved at pH 5 (0.5% DMSO in water) and is maintained for hours (Figure 2d). These conditions allow on demand photoconversion of the compound to the cyclic form but in an irreversible manner, i.e. no spontaneous back-conversion to the linear form is observed even at temperatures up to 50 ºC.

Reversible photoswitching can be achieved at higher DMSO concentration (20% in water at pH 5), which allows the colorless cyclic-DASA-barbital to spontaneously re-open in the dark and give the linear, colored form (tau ½ = 0.8 min) (Figure S9). Since the colored solution (containing a mixture of linear- and cyclic-DASA) is stable for hours in DMSO (Figure 2b), in 30% DMSO in water at pH 5 it can undergo multiple cycles of photoswitching and relaxation in the dark (tau ½ = 1.2 min) (Figure 2e). Although biological experiments generally cannot be performed in solutions containing more than 1% organic solvent, the reversible photoswitching of DASA-barbital observed over 20% DMSO hints that a hydrophobic environment can stabilize the colored form in the presence of water (Figure S10). Based on this evidence, we reasoned that a cage-complex approach[55] might afford transferring DASA-barbital in water and reversibly photoswitching it in physiological medium.

We used (2-hydroxypropyl)-β-cyclodextrin (HP-β-CD) as the complexing element to operate the photoswitch in pure water. Cyclodextrins are macrocycles of glucose subunits that are widely used to form inclusion complexes in drug formulation as delivery carriers due to their non toxicity.[56] The structure of β-cyclodextrin features a hydrophobic core (~7 Å diameter) and HP-β-CD is the hydroxyalkyl derivative, which gives improved water solubility and toxicology profile. HP-β-CD can accommodate the DASA compound and, thanks to its hydrophilic shell, allows its dispersion in water. Indeed, the solubility of DASA-barbital reaches mM concentrations in pure water with 25% w/v HP-β-CD (Figure S12). Remarkably, DASA-barbital can undergo reversible and repeatable cycles of photoswitching and thermal relaxation in pure water with 10% w/v of HP-β-CD in the formulation (Figure 2f). This result opens the way to using DASA derivatives in physiological media and to explore the application of this class of compounds in biology, which was deemed impossible so far.

To find out whether HP-β-CD stabilizes linear-DASA-barbital in aqueous environment following a similar mechanism to that observed with supramolecular vessels,[57,58] we examined the absorption spectra of the different formulations. The solvatochromism observed in the normalized UV-vis spectra of the molecule confirms that HP-β-CD immerse DASA-barbital in a hydrophobic environment (Figure 2g). The narrow peak of DASA-barbital at 615 nm in DMSO undergoes a hypsochromic shift when it is dissolved in water (pH 5 and 8, absorption maximum at 490 nm) and a bathochromic shift when HP-β-CD is added to the aqueous solution, yielding a maximum of 605 nm, near the value observed in the organic solvent (DMSO, absorption maximum at 615 nm).

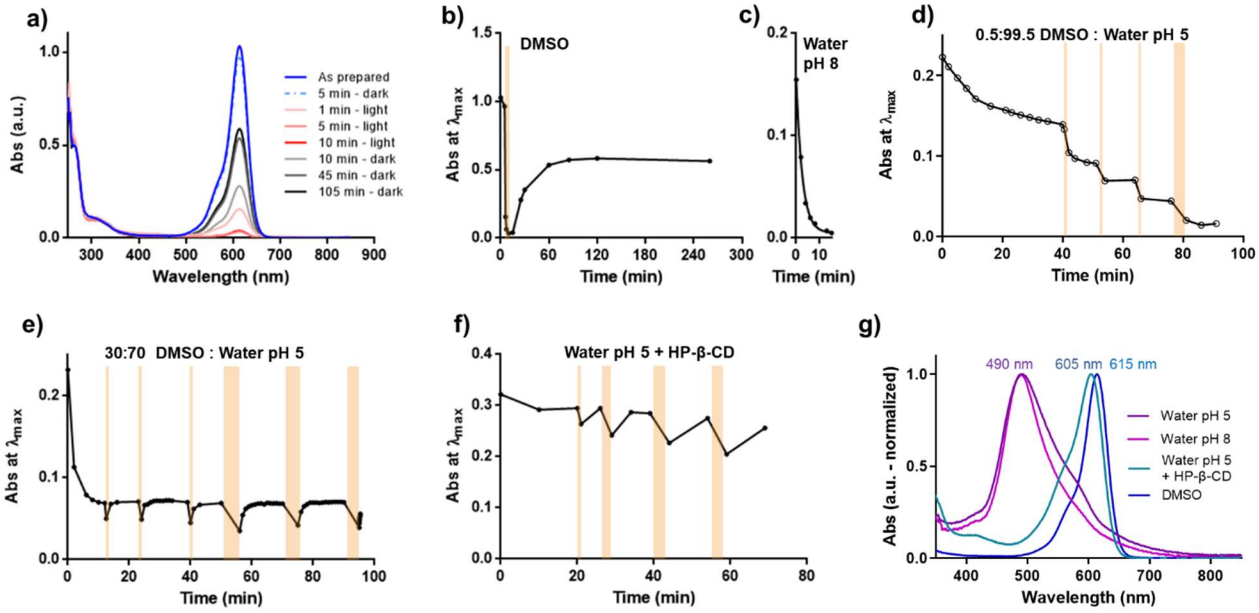

Figure 2. Reversible photoswitching of DASA-barbital in organic and aqueous media. a) UV/vis absorption spectra of 50 μM DASA-barbital in DMSO as prepared, after illumination with a halogen lamp, and after thermal relaxation in the dark. **b)** Time course of 50 μM DASA-barbital absorption at peak (615 nm) in DMSO under illumination (orange bar) and relaxation in the dark at room temperature. **c)** Spontaneous, irreversible conversion of 50 μM DASA-barbital in 0.5% DMSO:water at pH 8. **d)** Photo-induced irreversible conversion is possible with 50 μM DASA-barbital in 0.5% DMSO:water at pH 5. Time course at absorption peak (490 nm). **e)** Time course of 50 μM DASA-barbital during photoswitching cycles (1 or 5 min) in 30:70 DMSO:water at pH 5 at absorption peak (590 nm). **f)** Reversible photoswitching of 500 μM DASA-barbital in water at pH 5 can be achieved with 10% w/v HP-β-CD. Time course at absorption peak (605 nm) **g)** Normalized UV/vis absorption spectra of different solutions of DASA-barbital: water pH 5 (dark purple), water pH 8 (pink), DMSO (blue), and water and HP-β-CD 10% w/v pH 5 (light blue). DASA-barbital is thus exposed to a hydrophobic environment in HP-β-CD.

DASA-barbital is active in neurons *via* $GABA_A$ receptors.

Based on the close structural similarity between DASA-barbital and common barbiturate drugs (e.g. phenobarbital in Figure 1a), we asked whether it displays pharmacological activity in neurons. To measure the responses to drugs, we performed patch clamp electrophysiological recordings at pH 7.4 in 0.5% DMSO (note that HP-β-CD alone was observed to increase the neuron firing frequency and was not included in assays with DASA-barbital). Indeed, we observed that the firing frequency of cultured hippocampal neurons readily increases upon perfusion of 300 μM DASA-barbital (Figure 3a-e), whereas the vehicle only induces a slight decrease in the frequency (Figure 3b). We compared this behavior to that of phenobarbital, which blocks firing at 300 μM (Figure 3c), and to that of the $GABA_AR$ antagonist bicuculline (25 μM), which produces a similar response to DASA-barbital (Figure 3d). The increase in firing frequency induced by DASA-barbital suggests that it is an antagonist of $GABA_ARs$; however, this effect could also be caused by other ion channels and receptors that are expressed in hippocampal neurons.

To test whether the activity of DASA-barbital is directly mediated by $GABA_ARs$, we recorded GABAergic miniature inhibitory post synaptic currents (mIPSCs) in the presence of 1 μM tetrodotoxin (TTX) to block action potential-dependent release of GABA, and in the presence of glutamate receptors antagonists (10 μM 6-cyano-7-nitroquinoxaline-2,3-dione CNQX and 40 μM (2R)-amino-5-phosphonopentanoate APV) to block excitatory currents. Bath application of 300 μM DASA-barbital reduces the amplitude of $GABA_AR$-mediated synaptic currents by 55%, from 41 pA to 19 pA (see example trace in Figure 3f and quantification in Figure 3h; $n = 6$ cells; $p < 0.01$). In particular, the frequency of low amplitude events (below 20 pA) increases after application of DASA-barbital, and the events with amplitude higher than 60 pA disappear (Figure 3g). In addition, we tested whether DASA-barbital influences glutamatergic receptors by recording the amplitude of miniature excitatory post synaptic currents (mEPSCs) in the presence of 1 μM TTX and 25 μM bicuculline (see example trace in Figure 3i). The distribution and mean amplitude of the mEPSCs are not significantly altered upon bath application of 300 μM DASA-barbital (Figure 3jk, $n = 3$ cells, $p > 0.05$). Overall, these results demonstrate that the effect of DASA-barbital in neurons is primarily mediated by $GABA_ARs$ and that the compound is a pharmacological antagonist of these receptors.

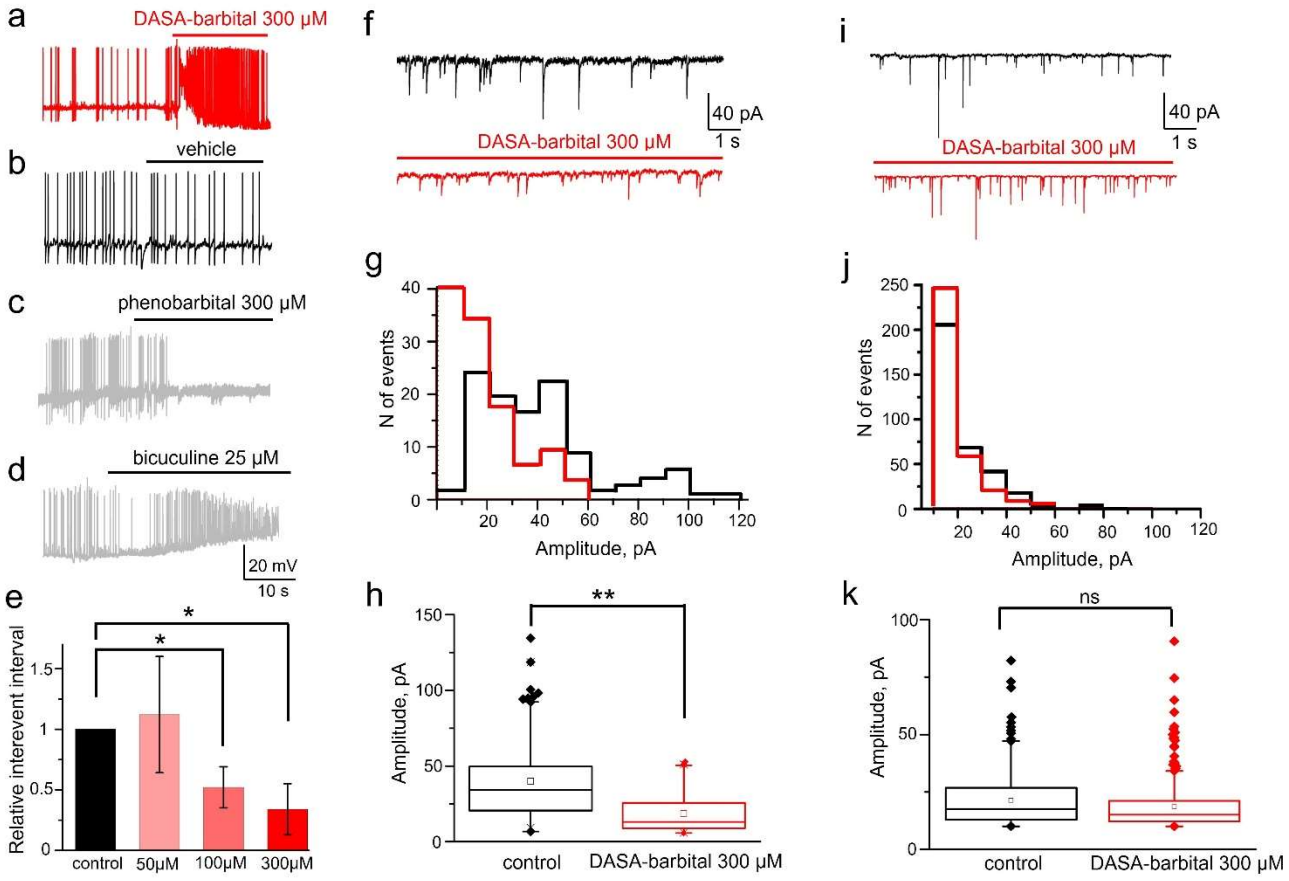

Figure 3. DASA-barbital is pharmacologically active in neurons and its effects are mediated by $GABA_A$Rs and not glutamate receptors. a. Application of 300 μM DASA-barbital increases the firing frequency of cultured hippocampal neurons. **b**. Application of the vehicle (0,5% DMSO, pH 7.4) does not increase neuronal firing. **c**. Application of 300 μM phenobarbital blocks action potential generation. **d**. Application of 25 μM bicuculline increases the neuronal firing frequency. **e.** Cumulative data showing the dose-dependent effect of DASA-barbital on the inter-event interval of neuronal action potentials (n=3 cells for each concentration, * - $p < 0,05$). **f**. Neuronal $GABA_A$R-mediated mIPSCs before (black trace) and during bath application of 300 μM DASA-barbital (red trace). **g**. Distribution of mIPSCs amplitudes before and after application of 300 μM DASA-barbital (black and red histograms, respectively). **h**. Box plot showing the effect of 300 μM DASA-barbital on the mean mIPSCs amplitude (n=6 cells, ** - $p < 0,01$). **i**. Neuronal glutamate receptor-mediated mEPSCs before and after application of 300 μM DASA-barbital (black and red traces, respectively). **j.** Distribution of mEPSCs amplitudes before and after application of 300 μM DASA-barbital (black and red histograms, respectively). **k**. Box plot showing that 300 μM DASA-barbital does not significantly alter the mean amplitude of mEPSCs (n=3 cells).

Discussion

Our results show that DASA-barbital is active in neurons *via* $GABA_AR$s, which raises exciting prospects for photopharmacology and neurobiology. Interestingly, receptor binding is retained in the cyclic form despite its bulky structure and the absence of branching, which is in contrast to most barbiturates.[52] The branching carbon is key to preserve the photochromism of DASAs regardless of the specific donor and acceptor groups chosen in future designs. Although barbiturates generally act as $GABA_AR$ potentiators, the antagonist character of DASA-barbital is also observed in structural analogs like bemegride,[59] and could be a useful tool in neurobiology as antidote or neurostimulant. Modification of propofol and benzodiazepine has also produced antagonists in some cases.[30,60,61] Different substitutions in the barbiturate ring of DASA-barbital (see below) might lead to compounds with agonist or potentiator properties that can be used as CNS inhibitors.

Besides their interest as neuroactive compounds, DASAs are widely appealing because they can be photoswitched with red and NIR light.[12,17,18] Compared to the UV light used in $GABA_AR$ photopharmacology so far,[30,60–62] the deep tissue penetration of longer wavelengths would overcome an important hurdle towards controlling neuronal activity noninvasively using transcranial illumination. Here, we have presented evidence of reversible photoswitching of DASA-barbital in water up to pH 5 and 10% HP-β-CD. Expanding these conditions to a range compatible with neuronal physiology (pH 7.4) is feasible and future experiments will aim at more hydrophilic and pH-independent DASA derivatives that can be reversibly photoswitched with low concentration of organic solvents and HP-β-CD. The rank of cyclodextrins as approved drug excipient is another compelling incentive in this quest.[53,63,64]

In conclusion, we have demonstrated for the first time that (1) the barbiturate acceptor group of DASA photoswitches is active in neuronal $GABA_AR$s and alters the firing rate of untransfected neurons in physiological medium at neutral pH, and (2) DASA-barbital can be reversibly photoswitched in acidic aqueous solutions compatible with drug formulations. Together, these contributions constitute a breakthrough to use native red activated DASAs in biology and to exploit their remarkable versatility displayed in polymers and materials science.

Methods

The procedures for DASA-barbital and phenobarbital synthesis, purification, chemical and photochemical characterization, primary hippocampal neuron culture, electrophysiological recordings and data analysis are described in the Supplementary Information section.

Acknowledgements

This research received funding from the European Union Research and Innovation Programme Horizon 2020 – Human Brain Project SG3 (945539), DEEPER (ICT-36-2020-101016787), Agency for Management of University and Research Grants/Generalitat de Catalunya (CERCA Programme; 2017-SGR-1442), Fonds Européen de Développement Économique et Régional (FEDER) funds, Ministry of Science and Innovation (Grant PID2019-111493RB-I00), Fundaluce and "la Caixa" foundations (ID 100010434, agreement LCF/PR/HR19/52160010). R.C. and G.M. were supported by the BEST Postdoctoral Fellowship, funded by the European Commission under H2020's Marie Sklowdoska-Curie Actions COFUND scheme (Grant Agreement no 712754) and by the Severo Ochoa programme of the Spanish Ministry of Science and Competitiveness (Grant SEV-2014-0425 (2015-2019)). R.C. acknowledges the European Regional Development Fund (ERDF) project PhOAMS (No.1.1.1.5/21/A/003). Mass spectrometry was performed at the IRB Barcelona Mass Spectrometry Core Facility, which actively participates in the BMBS European COST Action BM 1403 and is a member of Proteored, PRB2-ISCIII, supported by grant PRB2 (IPT13/0001—ISCIIISGEFI/FEDER).

References

1. Helmy, S. *et al.* Photoswitching using visible light: a new class of organic photochromic molecules. *J. Am. Chem. Soc.* **136**, 8169–72 (2014).

2. Helmy, S., Oh, S., Leibfarth, F. A., Hawker, C. J. & Alaniz, J. R. De. Design and Synthesis of Donor − Acceptor Stenhouse Adducts: A Visible Light Photoswitch Derived from Furfural. *J. Org. Chem.* **79**, 11316–11329 (2014).

3. Mason, B. P. *et al.* A temperature-mapping molecular sensor for polyurethane-based elastomers. *Appl. Phys. Lett.* **108**, (2016).

4. Lerch, M. M. *et al.* Solvent Effects on the Actinic Step of Donor–Acceptor Stenhouse Adduct Photoswitching. *Angew. Chemie - Int. Ed.* **57**, 8063–8068 (2018).

5. Lerch, M. M., Szymański, W. & Feringa, B. L. The (photo)chemistry of Stenhouse photoswitches: guiding principles and system design. *Chem. Soc. Rev.* (2018) doi:10.1039/C7CS00772H.

6. Singh, S. *et al.* Spatiotemporal Photopatterning on Polycarbonate Surface through Visible Light Responsive Polymer Bound DASA Compounds. *ACS Macro Lett.* **4**, 1273–1277 (2015).

7. Zhong, D., Cao, Z., Wu, B., Zhang, Q. & Wang, G. Polymer dots of DASA-functionalized polyethyleneimine: Synthesis, visible light/pH responsiveness, and their applications as chemosensors. *Sensors Actuators, B Chem.* **254**, 385–392 (2018).

8. Chen, Q. *et al.* Stable Activated Furan and Donor-Acceptor Stenhouse Adduct Polymer Conjugates as Chemical and Thermal Sensors. *Macromolecules* **52**, 4370–4375 (2019).

9. Jia, S., Fong, W. K., Graham, B. & Boyd, B. J. Photoswitchable Molecules in Long-Wavelength Light-Responsive Drug Delivery: From Molecular Design to Applications. *Chem. Mater.* **30**, 2873–2887 (2018).

10. Jia, S. *et al.* Investigation of Donor-Acceptor Stenhouse Adducts as New Visible Wavelength-Responsive Switching Elements for Lipid-Based Liquid Crystalline Systems. *Langmuir* **33**, 2215–2221 (2017).

11. Pianowski, Z. L. Recent Implementations of Molecular Photoswitches into Smart Materials and Biological Systems. *Chem. - A Eur. J.* **25**, 5128–5144 (2019).

12. Berraud-Pache, R. *et al.* Redesigning donor-acceptor Stenhouse adduct photoswitches through a joint experimental and computational study. *Chem. Sci.* **12**, 2916–2924 (2021).

13. Di Donato, M. *et al.* Shedding Light on the Photoisomerization Pathway of Donor-Acceptor Stenhouse Adducts. *J. Am. Chem. Soc.* **139**, 15596–15599 (2017).

14. Peterson, J. A., Stricker, F. & Read De Alaniz, J. Improving the kinetics and dark equilibrium of donor-acceptor Stenhouse adduct by triene backbone design. *Chem. Commun.* **58**, 2303–2306 (2022).

15. Hemmer, J. R. *et al.* Tunable Visible and Near Infrared Photoswitches. *J. Am. Chem. Soc.* **138**, 13960–13966 (2016).

16. Clerc, M. *et al.* Promoting the Furan Ring-Opening Reaction to Access New Donor–Acceptor Stenhouse Adducts with Hexafluoroisopropanol. *Angew. Chemie* **133**, 10307–10315 (2021).

17. Hemmer, J. R. *et al.* Controlling Dark Equilibria and Enhancing Donor-Acceptor Stenhouse Adduct Photoswitching Properties through Carbon Acid Design. *J. Am. Chem. Soc.* **140**, 10425–10429 (2018).

18. Martínez-López, D., Santamaría-Aranda, E., Marazzi, M., García-Iriepa, C. & Sampedro, D. π-Bridge Substitution in DASAs: The Subtle Equilibrium between Photochemical Improvements

and Thermal Control**. *Chem. - A Eur. J.* **27**, 4420–4429 (2021).

19. Xiong, C. *et al.* Carbon Spacer Strategy: Control the Photoswitching Behavior of Donor-Acceptor Stenhouse Adducts. *Langmuir* **37**, 802–809 (2021).

20. Lerch, M. M. *et al.* Solvent Effects on the Actinic Step of Donor–Acceptor Stenhouse Adduct Photoswitching. *Angew. Chemie - Int. Ed.* **57**, 8063–8068 (2018).

21. Sroda, M. M., Stricker, F., Peterson, J. A., Bernal, A. & Read de Alaniz, J. Donor–Acceptor Stenhouse Adducts: Exploring the Effects of Ionic Character. *Chem. - A Eur. J.* **27**, 4183–4190 (2021).

22. Mallo, N. *et al.* Photochromic switching behaviour of donor–acceptor Stenhouse adducts in organic solvents. *Chem. Commun.* **52**, 13576–13579 (2016).

23. Lerch, M. M., Wezenberg, S. J., Szymanski, W. & Feringa, B. L. Unraveling the Photoswitching Mechanism in Donor-Acceptor Stenhouse Adducts. *J. Am. Chem. Soc.* **138**, 6344–6347 (2016).

24. Wang, D. *et al.* Inducing molecular isomerization assisted by water. *Commun. Chem.* **2**, (2019).

25. Ash, C., Dubec, M., Donne, K. & Bashford, T. Effect of wavelength and beam width on penetration in light-tissue interaction using computational methods. *Lasers Med. Sci.* **32**, 1909–1918 (2017).

26. Ankenbruck, N., Courtney, T., Naro, Y. & Deiters, A. Optochemical Control of Biological Processes in Cells and Animals. *Angew. Chemie - Int. Ed.* **57**, 2768–2798 (2018).

27. Jia, S. & Sletten, E. M. Spatiotemporal Control of Biology : Synthetic Photochemistry Toolbox with Far-Red and Near-Infrared Light. *ACS Chem. Biol.* (2021) doi:10.1021/acschembio.1c00518.

28. Gorostiza, P. *et al.* Mechanisms of photoswitch conjugation and light activation of an ionotropic glutamate receptor. *Pnas* **104**, 10865–10870 (2007).

29. Mourot, A. *et al.* Tuning photochromic ion channel blockers. *ACS Chem. Neurosci.* **2**, 536–543 (2011).

30. Maleeva, G. *et al.* A photoswitchable GABA receptor channel blocker. *Br. J. Pharmacol.* **176**, 2661–2677 (2019).

31. Pittolo, S. *et al.* An allosteric modulator to control endogenous G protein-coupled receptors with light. *Nat. Chem. Biol.* **10**, 813–815 (2014).

32. Riefolo, F. *et al.* Optical Control of Cardiac Function with a Photoswitchable Muscarinic Agonist. *J. Am. Chem. Soc.* **141**, 7628–7636 (2019).

33. Prischich, D. *et al.* Adrenergic Modulation With Photochromic Ligands. *Angew. Chemie - Int. Ed.* **60**, 3625–3631 (2021).

34. Kaufman, H., Vratsanos, S. M. & Erlanger, B. F. Photoregulation of an enzymic process by means of a light-sensitive ligand. *Science (80-.).* **162**, 1487–1489 (1968).

35. Weston, C. E. *et al.* Toward Photopharmacological Antimicrobial Chemotherapy Using Photoswitchable Amidohydrolase Inhibitors. *ACS Infect. Dis.* **3**, 152–161 (2017).

36. Matera, C. *et al.* Photoswitchable Antimetabolite for Targeted Photoactivated Chemotherapy. *J. Am. Chem. Soc.* **140**, 15764–15773 (2018).

37. Velema, W. A. *et al.* Optical control of antibacterial activity. *Nat. Chem.* **5**, 924–928 (2013).

38. Jerca, F. A., Jerca, V. V. & Hoogenboom, R. Advances and opportunities in the exciting world of azobenzenes. *Nat. Rev. Chem.* **6**, 51–69 (2022).

39. Hüll, K., Morstein, J. & Trauner, D. In Vivo Photopharmacology. *Chem. Rev.* **118**, 10710–10747 (2018).

40. Crespi, S., Simeth, N. A. & König, B. Heteroaryl azo dyes as molecular photoswitches. *Nat. Rev. Chem.* **3**, 133–146 (2019).

41. Dong, M. *et al.* Near-Infrared Photoswitching of Azobenzenes under Physiological Conditions. *J. Am. Chem. Soc.* jacs.7b06471 (2017) doi:10.1021/jacs.7b06471.

42. Lentes, P. *et al.* Nitrogen Bridged Diazocines: Photochromes Switching within the Near-Infrared Region with High Quantum Yields in Organic Solvents and in Water. *J. Am. Chem. Soc.* **141**, 13592–13600 (2019).

43. Konrad, D. B. *et al.* Computational Design and Synthesis of a Deeply Red-Shifted and Bistable Azobenzene. *J. Am. Chem. Soc.* **142**, 6538–6547 (2020).

44. Cabré, G. *et al.* Rationally designed azobenzene photoswitches for efficient two-photon neuronal excitation. *Nat. Commun.* **10**, 907 (2019).

45. Pittolo, S. *et al.* Reversible silencing of endogenous receptors in intact brain tissue using 2-photon pharmacology. *Proc. Natl. Acad. Sci. U. S. A.* **116**, 13680–13689 (2019).

46. Izquierdo-Serra, M. *et al.* Two-photon neuronal and astrocytic stimulation with azobenzene-based photoswitches. *J. Am. Chem. Soc.* **136**, 8693–8701 (2014).

47. Kellner, S. & Berlin, S. Two-photon excitation of azobenzene photoswitches for synthetic optogenetics. *Appl. Sci.* **10**, (2020).

48. WHO, W. H. organization. *World Health Organization Model List of Essential Medicines*. *World Health Organization* vol. 22nd list https://www.who.int/publications/i/item/WHO-MHP-HPS-EML-2021.02 (2021).

49. Twyman, R. E., Rogers, C. J. & Macdonald, R. L. Differential regulation of γ-aminobutyric acid receptor channels by diazepam and phenobarbital. *Ann. Neurol.* **25**, 213–220 (1989).

50. Sigel, E. & Steinmann, M. E. Structure, function, and modulation of GABAA receptors. *J. Biol. Chem.* **287**, 40224–40231 (2012).

51. Ernst, J. B., Clark, G. F. & Grundman, O. The Physicochemical and Pharmacokinetic Relationships of Barbiturates – From the Past to the Future. *Curr. Pharm. Des.* **21**, 3681–3691 (2015).

52. Vardanyan, R. S. & Hruby, V. J. *Synthesis of Essential Drugs*. (2006).

53. Mallo, N. *et al.* Hydrogen-Bonding Donor-Acceptor Stenhouse Adducts. *ChemPhotoChem* **4**, 407–412 (2020).

54. Hoorens, M. W. H. & Szymanski, W. Reversible, Spatial and Temporal Control over Protein Activity Using Light. *Trends Biochem. Sci.* **43**, 567–575 (2018).

55. Upadhyay, R. K. Drug delivery systems, CNS protection, and the blood brain barrier. *Biomed Res. Int.* **2014**, (2014).

56. Gould, S. & Scott, R. C. 2-Hydroxypropyl-β-cyclodextrin (HP-β-CD): A toxicology review. *Food Chem. Toxicol.* **43**, 1451–1459 (2005).

57. Saha, R. *et al.* Unusual Behavior of Donor-Acceptor Stenhouse Adducts in Confined Space of a Water-Soluble PdII8 Molecular Vessel. *J. Am. Chem. Soc.* **141**, 8638–8645 (2019).

58. Payne, L., Josephson, J. D., Scott Murphy, R. & Wagner, B. D. Photophysical Properties of Donor-Acceptor Stenhouse Adducts and Their Inclusion Complexes with Cyclodextrins and Cucurbit[7]uril. *Molecules* **25**, (2020).

59. Mistry, D. & Cottrell, G. Actions of steroids and bemegride on the GABAA receptor of mouse spinal neurones in culture. *Exp. Physiol.* **75**, 199–209 (1990).

60. Lin, W. *et al.* Engineering a Light-Regulated GABAA Receptor for Optical Control of Neural Inhibition. *ACS Chem. Biol.* **9**, 1414–1419 (2014).

61. Lin, W. C. *et al.* A Comprehensive Optogenetic Pharmacology Toolkit for In Vivo Control of GABAA Receptors and Synaptic Inhibition. *Neuron* **88**, 879–891 (2015).

62. Rustler, K. *et al.* Optical Control of GABAA Receptors with a Fulgimide-Based Potentiator. *Chem. - A Eur. J.* **26**, 12722–12727 (2020).

63. Berry, M. H. *et al.* Restoration of patterned vision with an engineered photoactivatable G protein-coupled receptor. *Nat. Commun.* **8**, 1–12 (2017).

64. Lerch, M. M., Hansen, M. J., Velema, W. A., Szymanski, W. & Feringa, B. L. Orthogonal photoswitching in a multifunctional molecular system. *Nat. Commun.* **7**, 12054 (2016).